

# Diagnosis of PEM Fuel Cell Drying and Flooding Based on Power Converter Ripple

Giovanni Dotelli, Roberto Ferrero, *Member, IEEE*, Paola Gallo Stampino, Saverio Latorrata, and Sergio Toscani, *Member, IEEE*

## I. INTRODUCTION

**T**HE diffusion of fuel cell (FC) generators and in particular polymer electrolyte membrane (PEM) FCs is rapidly growing for stationary, mobile, and powertrain applications driven by the continuous progresses in FC technology. In this scenario, the development of control and diagnostic tools to guarantee proper operating conditions and improve the reliability of these systems is acquiring a fundamental importance [1].

One of the main issues that needs to be addressed for proper PEM FC operation is water management, as water content deeply affects the FC efficiency, stability, and lifetime. Indeed, a well-humidified membrane is essential to guarantee high conductivity and thus low-ohmic losses, but an excessive amount of water limits gas diffusion through the porous layers and therefore it reduces the output power as well [2], [3].

Manuscript received November 12, 2013; revised February 5, 2014; accepted April 10, 2014. Date of publication May 7, 2014; date of current version September 11, 2014. The Associate Editor coordinating the review process was Dr. Lorenzo Peretto.

G. Dotelli, P. G. Stampino, and S. Latorrata are with the Department of Chemistry, Materials, and Chemical Engineering G. Natta, Politecnico di Milano, Milan 20133, Italy (e-mail: giovanni.dotelli@polimi.it; paola.gallo@polimi.it; saverio.latorrata@polimi.it).

R. Ferrero is with the Department of Energy, Systems, Land and Constructions, University of Pisa, Pisa 56122, Italy (e-mail: roberto.ferrero@for.unipi.it).

S. Toscani is with the Dipartimento di Elettronica, Informazione e Bioingegneria, Politecnico di Milano, Milan 20133, Italy (e-mail: sergio.toscani@polimi.it).

An optimal tradeoff should then be found and maintained during operation to avoid performance decrease and damages to the cell.

Water balance in the FC is typically controlled by properly humidified input gases, but the relationship between gas humidity and the actual water content within the membrane and the gas diffusion layers is not straightforward, because of the variable water production rate at cathode depending on the current and on the complex transport mechanisms, such as electro-osmotic drag from anode to cathode and back-diffusion from cathode to anode [2].

The development of diagnostic methods to monitor the actual FC condition is therefore necessary to achieve a more effective humidity control, limiting the allowed variations and consequently the performance decrease and possible damages to the cell.

The most common diagnostic techniques allowing *in situ* measurements during FC operation are based on electrical measurements, which are little intrusive. Among these, electrochemical impedance spectroscopy (EIS) is generally recognized to provide the most complete information about the physical processes occurring within the FC [4], [5] and in particular it can well distinguish between the two opposite failure modes concerning the membrane humidity: 1) drying and 2) flooding [6]–[8]. Indeed, several diagnostic approaches based on it have been proposed in literature, e.g., [8]–[11]. However, the measurement of an impedance spectrum requires dedicated instrumentation, usually not available in commercial applications because of cost and system complexity issues.

On the other hand, most commercial applications include power converters (at least an inverter or a chopper) to connect the FC to the loads. These devices introduce a current ripple on the dc side, which is superimposed on the FC dc current. While some papers in literature (see [12]–[16]) have investigated the negative effects that such a ripple might produce on the FC (loss increase, possible damages, and durability decrease), little attention has been paid to the possibility to use this ripple as a diagnostic tool for monitoring the FC state-of-health by analyzing the FC response to this perturbation.

To the best of our knowledge, the use of power converter ripple for diagnostic purposes on PEM FCs was only reported by Mathias and Grot [17] and later by Hinaje *et al.* [18], with preliminary experimental results concerning a dc–dc converter ripple. The aim of these works was to use the high-frequency ripple to measure the FC ohmic resistance, which is a good indicator of the membrane humidity and can

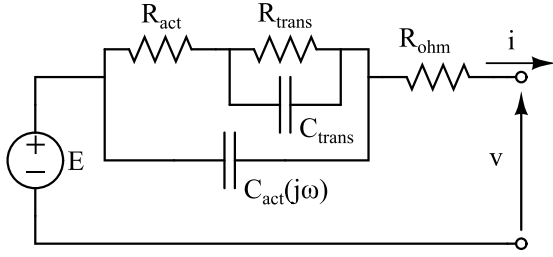


Fig. 1. Simplified linear equivalent circuit of a typical PEM FC.

therefore be employed to detect membrane drying. Despite the nonsinusoidal nature of the converter ripple, the analysis was carried out considering only the global amplitude of the current and voltage ripple waveforms.

In [19] the authors proposed a different approach, with a deeper analysis in the frequency domain to better estimate the ohmic resistance. Experimental results on a single PEM FC with a simulated three-phase inverter ripple showed that this method is able to provide an ohmic resistance value in agreement with the estimate obtained by classic EIS measurement. This paper further develops the experimental analysis, testing the ohmic resistance measurement during drying conditions and discussing the method sensitivity with respect to membrane dehydration. In addition, the possibility to effectively detect also flooding conditions by exploiting only the available ripple response is also discussed and tested as a new approach for their diagnosis.

## II. DIAGNOSTIC METHODS FOR DRYING AND FLOODING

Though the voltage–current relationship of a FC is not linear, a linear approximation can well describe most of the FC typical working conditions, excluding very low and very high currents. A simple linear model valid for small perturbations around a dc working point is shown in Fig. 1 in terms of equivalent electrical circuit. It considers all the three main causes of voltage drop, namely, activation polarization, mass transport limitation, and ohmic resistance [4].

Mass transport limitation, important at high current and low frequency, can be modeled in a first approximation by a  $RC$  circuit ( $R_{trans}$  and  $C_{trans}$  in the figure), although more complex models can be found in literature involving, e.g., the Warburg impedance [4]. Similarly, also the activation polarization can be modeled by a  $RC$  circuit ( $R_{act}$  and  $C_{act}$ ), but in this case a significant frequency dependence of the capacitance should be considered, either replacing the capacitance by a constant-phase element [4] or using a Debye-like model for the capacitance [15]

$$C_{act}(j\omega) = C_{act,\infty} + \frac{C_{act,s} - C_{act,\infty}}{1 + j\omega\tau_d} \quad (1)$$

being  $C_{act,s}$  and  $C_{act,\infty}$  the low and high frequency limit capacitance values and  $\tau_d$  the equivalent time constant. Finally, the ohmic voltage drop, mainly associated with the flow of ions through the membrane, is described by the resistance  $R_{ohm}$ .

As far as drying and flooding conditions are concerned, they both have significant impact on the FC impedance spectrum [6]–[8]. In the present technologies which mainly utilize

perfluorosulfonic acid membranes (Nafion is the prototypical example), the membrane conductivity is very sensitive to water content, therefore membrane dehydration causes a significant increase of the ohmic resistance. On the other hand, flooding of porous layers (gas diffusion layer and catalyst layer) limits the gas transport through these layers, so that the low-frequency  $R_{trans}C_{trans}$  arc in the Nyquist plot of the impedance spectrum significantly grows.

The EIS is therefore a suitable nonintrusive technique to detect both drying and flooding. However, it requires dedicated and expensive instrumentation (e.g., a frequency response analyzer), able to impose sinusoidal perturbations over a wide frequency range and to evaluate the FC impedance spectrum from the measured response. In a commercial application, such instrumentation would often require an unacceptable increase of cost and system complexity (volume and weight might also be critical for portable applications). It is worth noting that the FC voltage measurement alone is not sufficient, as it can only reveal a performance decrease but it cannot distinguish between drying and flooding [8]. Thus, alternative solutions have to be investigated.

As far as ohmic resistance is concerned, several measurement methods are known and commonly employed [20]. The simplest one from the implementation point of view, as it does not require dedicated instrumentation, is the current interruption: the measurement of the sudden voltage variation  $\Delta V = R_{ohm}I$  due to current interruption theoretically provides the value of the ohmic resistance. However, in practice the ohmic voltage variation could be not easily recognizable because of the inductive response of the circuit to fast current transients. In addition, the current interruption is quite intrusive for the FC, making such a measurement not suitable for frequent repetition.

A less intrusive method, known as high-frequency resistance (HFR) measurement, evaluates the ohmic resistance from the FC response to a small high-frequency sinusoidal perturbation. This technique is similar to EIS, but it is faster because it only measures the impedance at a single-frequency, which has to be properly chosen so that the FC impedance equals the ohmic resistance, otherwise significant errors might arise. The problem for commercial applications remains the requirement of dedicated instrumentation, unless the ripple of power converters is used as suggested in [17] and [18]. However, in this case, a correct choice of the excitation frequency becomes practically impossible, considering that the optimal value is likely to change during operation, while the switching frequency cannot follow such changes. Therefore, the nonsinusoidal nature of the ripple and the nonperfectly resistive behavior of the FC should be considered for a better estimate of the ohmic resistance, as will be discussed in Section IV-A.

On the other hand, the identification of flooding conditions by means of electrical measurements requires to analyze the low-frequency response of the FC, either by acquiring the complete spectrum [8] or the response to a single-frequency perturbation in the frequency range where transport dynamics is visible (typically below 10 Hz) [9]. In both cases, dedicated instrumentation is needed, because power converter ripple is

in a higher frequency range and thus it cannot be used for this purpose. Actually, the power electronics converter can be controlled to inject low-frequency components, as required by many diagnostic techniques in other fields [21]. However, the control becomes more complicated, the presence of the additional ripple increases the power losses and may also disturb the electrical load.

For this reason, nonelectrical methods are often used as alternative solutions to diagnose FC flooding [22]. Among these, the most suitable technique for commercial applications is based on pressure drop measurements, particularly at the cathode side. The presence of liquid water in the porous layers reduces the available area for gas diffusion, which in turn leads to a pressure drop increase [3], [23], [24]. In this paper, the possibility to diagnose FC flooding from the high-frequency impedance measurements provided by the power converter ripple response together with the dc voltage measurement is discussed, suggesting a possible diagnostic algorithm suitable for low-cost humidity control (see Section IV-B).

### III. POWER CONVERTER RIPPLE

The typical  $V-I$  characteristic of a FC is very different from that of a conventional battery of similar power rating which behaves like a dc voltage source with a small series resistance. When a FC operates near the maximum rated power, its output voltage drops considerably. Because of this, a proper power converter which controls the output voltage is always needed even when the FC is connected to a dc load. In addition, in many cases even a dc-ac conversion is needed, since a lot of promising applications, such as vehicles and grid-connected generators, require an ac voltage supply.

A great number of power electronics converters for FC applications have been proposed in literature and the choice of the topology strictly depends on the stack output voltage, the output power, the type of load, and other peculiarities [25]. When the focus is moved on ac applications, the converters can be roughly classified into single-stage and two-stage. Two-stage converters are basically made of a dc-dc converter which controls the voltage fed to the dc-ac output converter, while a single-stage converter is basically an inverter whose dc side voltage may significantly change.

The two-stage converter is usually employed in small stacks, when the output voltage of the FC is not greater than the maximum ac voltage. In this case, the dc-dc stage boosts the voltage other than controlling its amplitude and it may include a high-frequency transformer that provides the galvanic insulation between load and FC. A two-stage solution often results in reduced stresses to the load and better control performance, but suffers from higher complexity and cost [26]. In any case, whatever power converter is chosen, the current flowing through the FC contains a small, high-frequency ripple, which is due to the commutations of the electronic switches.

This paper is focused on single stage dc-ac converters as a case study, but the results presented in the following sections are quite general. The proposed diagnostic method just requires a high-frequency ripple having a well-known frequency superimposed on the FC current. However, it should

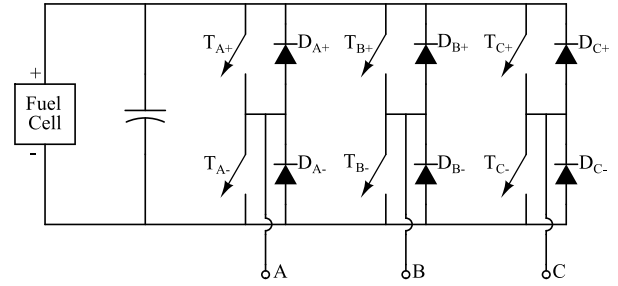


Fig. 2. Schematic representation of a three-phase inverter connected to the FC.

be noted that the ripple waveform might affect the uncertainty of the measurements since it depends on the harmonic content. For example, if a two-stage conversion were considered, with a boost PWM chopper connected to the FC, the current ripple would be mainly determined by the dc-dc conversion stage and in this case it would be a triangular waveform whose shape changes according to the duty cycle [18]. Although in the time domain the current ripple is very different from that produced by a PWM inverter having the same switching frequency, the frequencies of their harmonic components are not so different, since most of them are located near the multiples of the switching frequency.

Now, let us consider a dc-ac converter connected to the FC, and let us assume that the system operates in steady state conditions. In addition to the high-frequency ripple due to the switching, the FC current may contain also lower frequency components which depend on the inverter topology, on the output frequency and on the load characteristics. In particular, the power drawn by single-phase inverters or three-phase inverters connected to unbalanced loads contains an alternating component at twice the ac output frequency (for example, 100/120 Hz in 50/60 Hz systems) which is not present in case of three-phase inverters feeding balanced loads. In turn, a spectral component having the same frequency appears in the FC current, and it may be used to estimate the FC impedance at this frequency.

This paper discusses the possibility to exploit the FC current ripple to detect cell drying and flooding through two case studies. In the first one, the FC is connected to a three-phase inverter feeding a balanced load. The switches are controlled using the well-known sinusoidal pulse width modulation technique. A schematic representation of the inverter circuit is shown in Fig. 2. The carrier signal used to control the switching devices is a 1-kHz triangular waveform and the voltage control signals are three 50-Hz sine waves with  $2\pi/3$  shift from each other. For simplicity, also the inverter output currents are assumed to be ideal sine waves with  $2\pi/3$  shift from each other and the load is assumed to be resistive. Thus, the inverter input current has its main harmonic components around the switching frequency and its multiples. The current ripple superimposed on the FC current is clearly filtered thanks to the dc link capacitance; for this case study, it was designed to reduce the residual rms ripple to 3% of the dc current, which is an acceptable value for a FC [12], [25].

In the second case study, the cell is connected to a PWM single-phase inverter having a 1-kHz switching frequency.

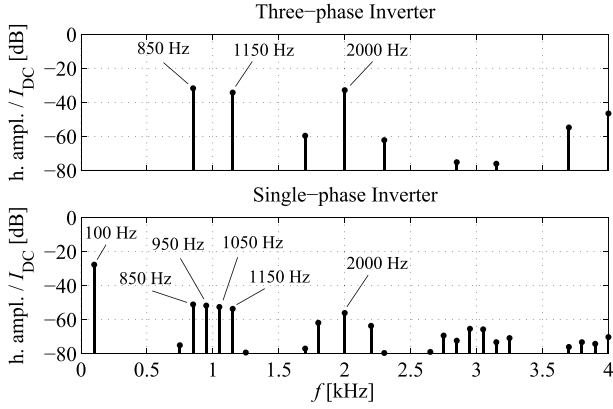


Fig. 3. Current spectra of the three-phase (upper plot) and single-phase (lower plot) inverter ripples considered as case studies.

Even in this case, a resistive load has been supposed, while the ac current is a 50-Hz sine wave. The dc link capacitance limits the residual rms ripple to 3% of the dc current, which is in most part due to the alternating power consumption of the single-phase load. The current spectra for the two case studies are shown in Fig. 3.

#### IV. PROPOSED MEASUREMENT METHOD

##### A. Ohmic Resistance Measurement

As discussed in the previous section, the current ripple waveform contains several high-frequency harmonic components. However, because of the low-pass effect of the dc link capacitance, only the lowest order components of the FC current ripple (highlighted in Fig. 3 for the considered case studies) have a significant amplitude, thus allowing accurate impedance measurements.

At these frequencies the FC response is linear and the voltage waveform produced by the current ripple contains the same harmonic components of the current. Therefore, if the Fourier transform is applied to both current and voltage signals, the impedance value can be calculated for each frequency as complex voltage–current ratio. Though even a single-frequency measurement could often provide a rough estimate of the ohmic resistance according to the HFR measurement method mentioned in Section II, the multifrequency nature of the ripple waveform can be exploited to perform a better measurement of it by fitting the experimental data with a suitable model.

As an example, with the considered switching frequency (1 kHz), good results can be usually obtained with a first-order capacitive model, derived from the general model of Fig. 1 by neglecting the transport dynamics and the frequency dependence of the activation polarization, that are not important at the ripple frequencies, thus leading to

$$Z(j\omega) = R_{\text{ohm}} + \frac{R_{\text{eq}}}{1 + j\omega R_{\text{eq}} C_{\text{eq}}} \quad (2)$$

where  $R_{\text{ohm}}$  is the ohmic resistance, while  $R_{\text{eq}}$  and  $C_{\text{eq}}$  represent the high-frequency equivalent circuit for activation polarization. An example of data fitting with this model is shown in Fig. 4 for the three-phase inverter case.

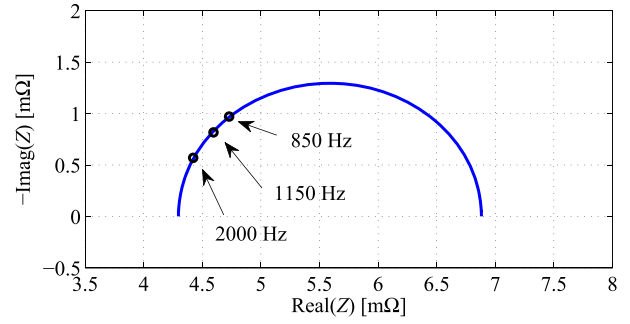


Fig. 4. Fit of the high-frequency impedance measurements to estimate the ohmic resistance value, according to the proposed method, for the three-phase inverter case.

It is worth noting that a different switching frequency, as well as different cutoff frequencies of the FC equivalent circuit, could require different (and maybe more complex) models to fit the experimental data, but the advantages of the fit compared with a single-frequency measurement still remain. The 1-kHz switching frequency was chosen as a suitable example to illustrate the proposed method (though higher switching frequencies are likely to be employed in many applications), because at this frequency the FC response mainly depends on its internal processes, whereas inductive effects due to electrical connections might arise at higher frequencies. Since they vary from case to case, the analysis and the consequent considerations would become less general.

##### B. Discrimination Between Drying and Flooding

While the ohmic resistance measurement represents a good indicator for membrane dehydration, it cannot be used to detect flooding because, when the membrane is fully hydrated, a further increase in the water content does not produce any significant change in the ohmic resistance. Nevertheless, the combined monitoring of ohmic resistance and dc voltage can be used in a model-based diagnostic algorithm to indirectly recognize flooding.

In more details, when a FC voltage drop is observed in stationary working conditions (i.e., constant dc current, cell temperature, and gas flow rates), it means that a change occurred either in ohmic resistance, activation polarization or transport limitation. If the ohmic resistance measurement reveals no change, at least one of the other two causes is responsible for the observed voltage drop.

In several applications, it is possible to *a priori* exclude any significant change of the activation polarization in a short time. In such a case, drying and flooding can be discriminated without additional information. On the other hand, there are other applications in which particular degradation situations might occur, affecting activation processes. Among these, Pt-catalyst layer poisoning due to the presence of CO in the hydrogen stream [6], [27] or chlorides in the air stream [28] are prototypical examples of phenomena leading to a dramatic charge transfer resistance increase without affecting membrane resistance, while ammonia in the air stream causes a simultaneous change of membrane and charge transfer resistances [29].

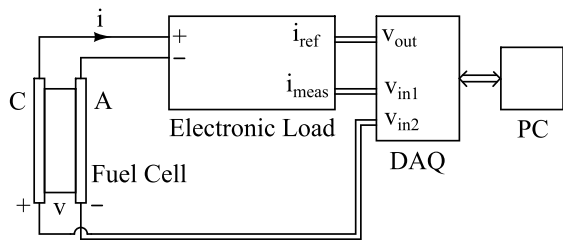


Fig. 5. Diagram of the measurement circuit.

The proposed approach to discriminate between drying and flooding conditions in such situations when also charge transfer resistance variations are possible, is to use the low-frequency inverter ripple (when present) to monitor the FC impedance at 100/120 Hz. This frequency is in the typical range of activation dynamics and it has therefore a high sensitivity with respect to charge transfer resistance variations. In more details, the imaginary part of the impedance is monitored, so that it is not affected by variations of the ohmic resistance, that only shifts the impedance spectrum along the real axis.

It is worth noting that, as said before, the ripple at twice the inverter output frequency is introduced by single-phase inverters and by three-phase inverters connected to unbalanced loads, but it can be easily generated also in three-phase inverters feeding a balanced load by superimposing a small negative sequence component to the output voltage.

## V. EXPERIMENTAL ANALYSIS

### A. Experimental Setup

The use of inverter current ripple for FC diagnostics is clearly intended for commercial applications in which stacks of several cells are employed. However, to better explain the proposed technique and to evaluate whether it is able to provide meaningful results, the three-phase and single-phase inverter current waveforms described in Section III were generated by a multifunction 16-bit data acquisition (DAQ) system (NI 6251) and applied to a single PEM FC (Fuel Cell Technologies) through an electronic load (TDI RBL488-50-150-800). A diagram of the measurement circuit is shown in Fig. 5.

The cell has a 23-cm<sup>2</sup> area and it is composed of commercial materials, in particular a Nafion 212 membrane as electrolyte (50- $\mu$ m thickness) and a gas diffusion electrode reference sample (E-TEK LT140). It was fed with pure hydrogen and air at the anode and cathode, respectively, with nominal flow rates of 0.2 NI/min for hydrogen and 1.0 NI/min for air, measured and controlled by calibrated flow meters. The cell temperature was kept constant at 60 °C, while the relative humidities of the input gases were controlled by saturators. A photograph of the experimental setup is shown in Fig. 6.

A typical impedance spectrum at medium current ( $I_{dc} = 11.5$  A, corresponding to 0.5 A/cm<sup>2</sup>) is shown in Fig. 7, measured by a frequency response analyzer (Solartron 1260) in the frequency range from 0.5 Hz to 1 kHz. The impedance values are fitted by the equivalent circuit model in Fig. 1,

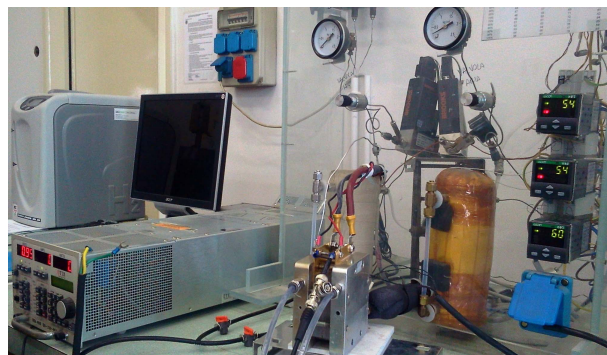


Fig. 6. Photograph of the experimental setup.

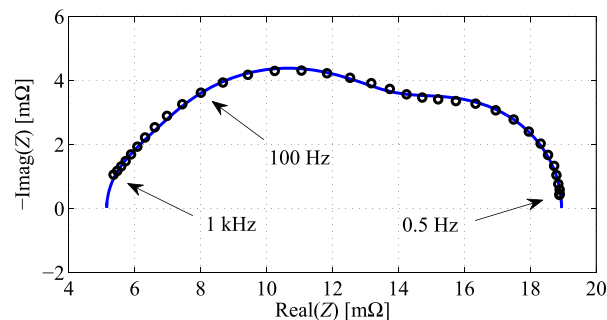


Fig. 7. Impedance spectrum of the FC under test in nominal working condition: experimental data (circles) and best fit obtained with the model in Fig. 1 (solid line).

showing good agreement between model and experimental data. The impedance measurement at 100 Hz is highlighted in the figure to verify that it belongs to the high-frequency arc of the Nyquist plot, associated with activation dynamics.

For the experimental analysis reported in this paper, the cell voltage and the current measurement signal provided by the electronic load were acquired by the same DAQ system used for signal generation, with  $5 \cdot 10^5$  samples-per-second sampling frequency. The measured current and voltage waveforms in case of the three-phase inverter ripple are reported in Fig. 8. The voltage Fourier spectrum confirms that the FC response at these frequencies is linear, as it contains the same harmonic components of the current, thus allowing to apply the superposition principle to evaluate the impedance values at the different frequencies. The response linearity represents an important advantage because it allows to use any available ripple (even with significant amplitude, if it is allowed by other design requirements), without any concern about the validity of the measured frequency response. This is still valid also if the 100 Hz component is present in the ripple waveform.

The possibility to employ the changes of the impedance to detect malfunctions of the FC is strictly related to the measurement resolution more than the measurement uncertainty. In turn, resolution is limited because of the noise, which is due to the measurement system but also to the measurand and to the fluctuations of the influence quantities. *A priori* evaluation is very difficult, therefore a statistical approach has been chosen. The measurement of the impedances corresponding to the frequencies excited by the FC current ripple has been

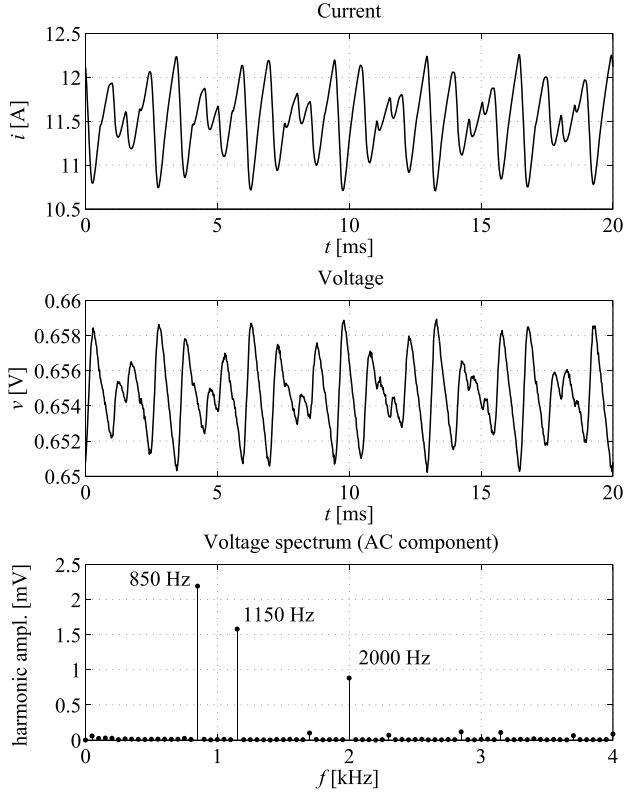


Fig. 8. Measured current and voltage waveforms (upper and middle plots) and Fourier spectrum of the ac voltage component (lower plot), in one period of the three-phase inverter ripple.

repeated, while the FC operates in stationary conditions. The noise level is represented by the standard deviation of the impedance magnitude, and in each condition is well below 0.1 m $\Omega$ . Therefore, variations greater than this are significant since they are not masked by noise.

### B. Drying Conditions

FC drying was obtained by gradually decreasing the input gas relative humidity (at both anode and cathode) by acting on the saturator temperatures. Since the most significant effects appear at low current due to the lower water production by the chemical reaction at cathode, the tests were performed at a medium-low current ( $I_{dc} = 9$  A).

For a rough evaluation of the expected ohmic resistance variations when the membrane is dehydrated, a preliminary test was carried out to measure the experimental curve of  $R_{ohm}$  versus the input gas relative humidity in stationary conditions, shown in Fig. 9. The relative humidity was decreased from 85% (corresponding to a well-hydrated membrane) to 55% with step-wise variations and, for each measurement, the cell was run for 1 h after the saturator temperature was changed to reach a stationary condition. After this waiting time, the dc voltage and ohmic resistance were measured for 5 min, so that the mean value and the standard deviation could be calculated. The higher standard deviations observed at low humidities are due to natural ohmic resistance oscillations that appear when the membrane is not fully humidified [30]. The voltage measurements are also reported in the figure to

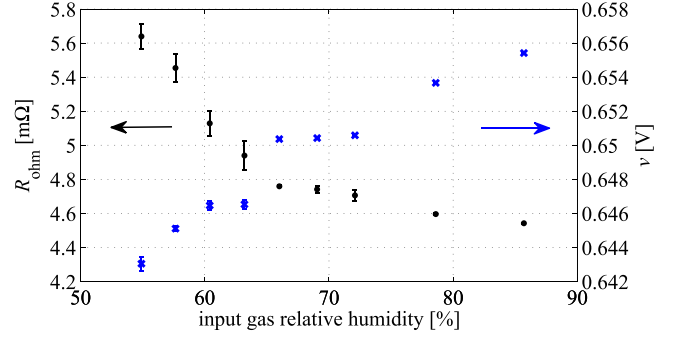


Fig. 9. Voltage (blue crosses) and ohmic resistance (black dots) variations versus input gas relative humidity; the vertical bars represent the standard deviations of the measured quantities during the measurement time.

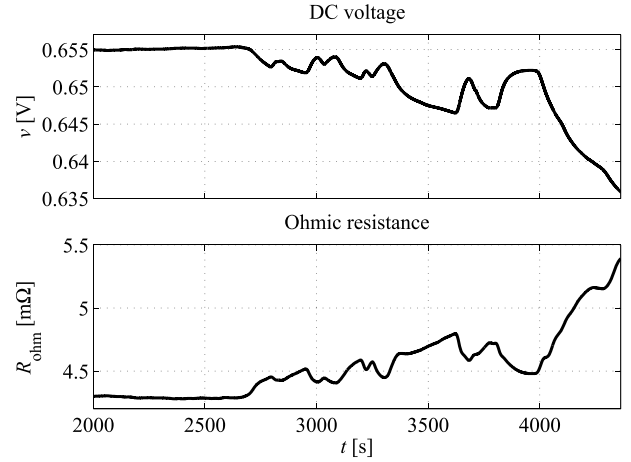


Fig. 10. Voltage (upper plot) and ohmic resistance (lower plot), measured with the three-phase inverter ripple during a drying transient.

show the smaller relative variations and the less regular shape compared with the resistance–humidity characteristics, that make the latter more suitable to detect drying.

To test the proposed method for drying diagnosis, the FC ohmic resistance was monitored from the three-phase inverter ripple as explained in Section IV-A (but a single-phase inverter would be equally suitable for this purpose), while the input gas humidity was gradually decreased from 100% to 60%, by diminishing the saturator temperature. The measured dc voltage and ohmic resistance after 2000 s from the beginning of the test are reported in Fig. 10 (the signals are low-pass filtered to better highlight the slow variations). The long time before the ohmic resistance starts to increase is justified by the very slow thermal and transport dynamics that links the saturator temperature to the membrane humidity. While the water content is enough for a full membrane hydration, the ohmic resistance remains approximately constant [30], then it suddenly starts to increase, and consequently the voltage starts to decrease proportionally to it. The low uncertainty of the ohmic resistance measurement and its high sensitivity with respect to membrane dehydration allow to promptly recognize drying long before a great voltage decrease occurs.

It is important to note that the curve of  $R_{ohm}$  versus the input gas relative humidity shown in Fig. 9 cannot be used here to estimate the input gas humidity from the ohmic resistance

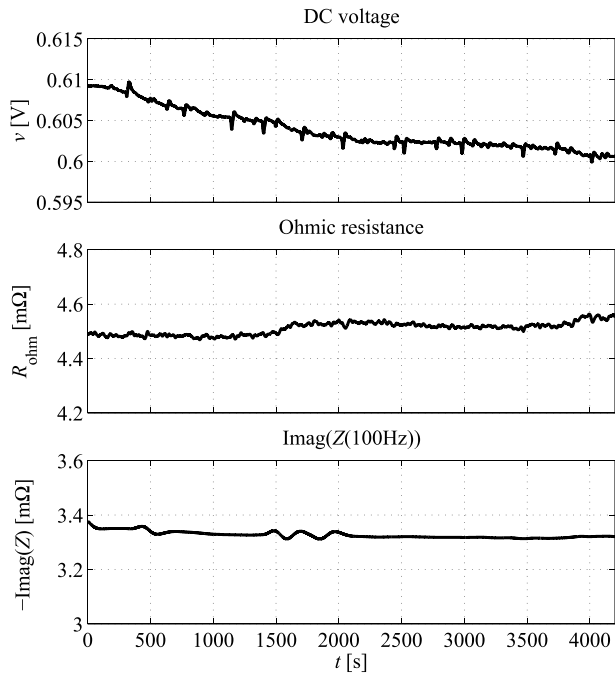


Fig. 11. Voltage (upper plot), ohmic resistance (middle plot), and imaginary part of the impedance at 100 Hz (lower plot), measured with the single-phase inverter ripple during a flooding transient.

measurement, since the curve was obtained in stationary conditions and it does not apply to transients like the one in Fig. 10. However, this is not important because the aim of the proposed diagnostic method is not to estimate the gas humidity, but only to sense ohmic resistance variations, that can be eventually used in a feedback control to restore the nominal conditions, when possible.

### C. Flooding Conditions

Conversely to what done for membrane dehydration, FC flooding was obtained by increasing the input gas relative humidity over the saturation value and reducing the gas flow rates (0.08 Nl/min for hydrogen and 0.31 Nl/min for air) to decrease water removal. The test was performed in the same working point used for drying conditions ( $I_{dc} = 9$  A) to better compare the two transients.

According to the diagnostic algorithm proposed in Section IV-B, the single-phase inverter ripple was chosen for this test, so that the impedance at 100 Hz could be monitored as well as the ohmic resistance, although the three-phase inverter could have also been employed in this case, since variations of activation processes can be *a priori* excluded here. The continuous voltage decrease observed for about 4000 s from the beginning of the test is reported in Fig. 11, together with the ohmic resistance measurement and the imaginary part of the 100-Hz impedance (again, the signals are filtered by a low-pass filter). It should be noted that in flooding transients the FC voltage waveform is affected by fast spikes (only partially recognizable in the filtered signal), corresponding to sudden voltage drops probably due to temporary flooding of gas channels, which in turn give rise to consequent slower transients on time scales of several tens of seconds [31].

From Fig. 11, it can be seen that neither the ohmic resistance nor the imaginary part of the 100-Hz impedance show significant variations during the selected measurement time, thus excluding ohmic losses and activation polarization as possible causes of the observed voltage drop. This means that transport limitations are responsible for it, for which flooding is the most probable cause if the input gas pressures and flow rates are constant.

## VI. CONCLUSION

A method for monitoring the state-of-health of a PEM FC was presented, suitable for *in situ* measurements in commercial applications, where cost and system complexity issues usually prevent from performing standard EIS measurements with dedicated instrumentation. The proposed method exploits the current ripple introduced by switch mode power converters to identify the FC impedance spectrum in the high-frequency range.

The main novelty of the technique presented in this paper, compared with similar works on this topic, is the frequency-domain analysis that allowed to identify the impedance values at different frequencies and from them to calculate a better estimate of the FC ohmic resistance through data fitting, thus obtaining a good indicator of the membrane water content. Furthermore, the monitoring of the 100/120-Hz impedance from low-frequency ripple is proposed as a possible approach to discriminate between flooding and drying based only on the available impedance and dc voltage measurements, in those applications where degradation conditions affecting the activation processes (e.g., Pt-catalyst layer poisoning) can also occur.

The proposed technique was experimentally tested on a single PEM FC by emulating the current ripple due to three-phase and single-phase PWM inverters. Though the tests involved only two possible ripple waveforms, it is opinion of the authors that this technique can be applied also in case of different PWM-controlled power converter topologies, as long as they produce a ripple of the FC current with a sufficient spectral content at the frequencies of interest.

## REFERENCES

- [1] J. Wu, X. Z. Yuan, H. Wang, M. Blanco, J. J. Martin, and J. Zhang, "Diagnostic tools in PEM fuel cell research: Part I Electrochemical techniques," *Int. J. Hydrogen Energy*, vol. 33, no. 6, pp. 1735–1746, 2008.
- [2] W. Dai *et al.*, "A review on water balance in the membrane electrode assembly of proton exchange membrane fuel cells," *Int. J. Hydrogen Energy*, vol. 34, no. 23, pp. 9461–9478, 2009.
- [3] N. Yousfi-Steiner, P. Moçotéguy, D. Candusso, D. Hissel, A. Hernandez, and A. Aslanides, "A review on PEM voltage degradation associated with water management: Impacts, influent factors and characterization," *J. Power Sour.*, vol. 183, no. 1, pp. 260–274, 2008.
- [4] X. Z. Yuan, C. Song, H. Wang, and J. Zhang, *Electrochemical Impedance Spectroscopy in PEM Fuel Cells*. London, U.K.: Springer-Verlag, 2010.
- [5] X. Yuan, H. Wang, J. C. Sun, and J. Zhang, "AC impedance technique in PEM fuel cell diagnosis—A review," *Int. J. Hydrogen Energy*, vol. 32, no. 17, pp. 4365–4380, 2007.
- [6] J. M. Le Canut, R. M. Abouatallah, and D. A. Harrington, "Detection of membrane drying, fuel cell flooding, and anode catalyst poisoning on PEMFC stacks by electrochemical impedance spectroscopy," *J. Electrochem. Soc.*, vol. 153, no. 5, pp. A857–A864, 2006.

- [7] W. Mérida, D. A. Harrington, J. M. L. Canut, and G. McLean, "Characterisation of proton exchange membrane fuel cell (PEMFC) failures via electrochemical impedance spectroscopy," *J. Power Sour.*, vol. 161, no. 1, pp. 264–274, 2006.
- [8] N. Fouquet, C. Doulet, C. Nouillant, G. Dauphin-Tanguy, and B. Ould-Bouamama, "Model based PEM fuel cell state-of-health monitoring via ac impedance measurements," *J. Power Sour.*, vol. 159, no. 2, pp. 905–913, 2006.
- [9] T. Kurz, A. Hakenjos, J. Krämer, M. Zedda, and C. Agert, "An impedance-based predictive control strategy for the state-of-health of PEM fuel cell stacks," *J. Power Sour.*, vol. 180, no. 2, pp. 742–747, 2008.
- [10] P. Kurzweil and H. J. Fischle, "A new monitoring method for electrochemical aggregates by impedance spectroscopy," *J. Power Sour.*, vol. 127, nos. 1–2, pp. 331–340, 2004.
- [11] S. K. Roy and M. E. Orazem, "Analysis of flooding as a stochastic process in polymer electrolyte membrane (PEM) fuel cells by impedance techniques," *J. Power Sour.*, vol. 184, no. 1, pp. 212–219, 2008.
- [12] R. S. Gemmen, "Analysis for the effect of inverter ripple current on fuel cell operating condition," *J. Fluids Eng.*, vol. 125, no. 3, pp. 576–585, 2003.
- [13] W. Choi, J. W. Howze, and P. Enjeti, "Development of an equivalent circuit model of a fuel cell to evaluate the effects of inverter ripple current," *J. Power Sour.*, vol. 158, no. 2, pp. 1324–1332, 2006.
- [14] B. Wahdame, "Impact of power converter current ripple on the durability of a fuel cell stack," in *Proc. IEEE ISIE*, Cambridge, U.K., Jul. 2008, pp. 1495–1500.
- [15] R. Ferrero, M. Marracci, M. Prioli, and B. Tellini, "Simplified model for evaluating ripple effects on commercial PEM fuel cell," *Int. J. Hydrogen Energy*, vol. 37, no. 18, pp. 13462–13469, 2012.
- [16] R. Ferrero, M. Marracci, and B. Tellini, "Single PEM fuel cell analysis for the evaluation of current ripple effects," *IEEE Trans. Instrum. Meas.*, vol. 62, no. 5, pp. 1058–1064, May 2013.
- [17] M. F. Mathias and S. A. Grot, "System and method for controlling the humidity level of a fuel cell," U.S. Patent 6376111, Apr. 23, 2002.
- [18] M. Hinaje, I. Sadli, J. P. Martin, P. Thounthong, S. Raël, and B. Davat, "Online humidification diagnosis of a PEMFC using a static DC–DC converter," *Int. J. Hydrogen Energy*, vol. 34, no. 6, pp. 2718–2723, 2009.
- [19] G. Dotelli, R. Ferrero, P. G. Stampino, and S. Latorrata, "Inverter ripple as a diagnostic tool for ohmic resistance measurements on PEM fuel cells," in *Proc. IEEE AMPS 2013*, Aachen, Germany, Sep., pp. 156–161.
- [20] K. R. Cooper and M. Smith, "Electrical test methods for on-line fuel cell ohmic resistance measurement," *J. Power Sour.*, vol. 160, no. 2, pp. 1088–1095, 2006.
- [21] S. L. Ho and K. W. E. Cheng, "Condition monitoring of rotor faults in induction motors by injection of low frequency signals into the supply," in *Proc. Power Electronics and Variable Speed Drives*, Sorrento, Italy, Sep. 1998, pp. 200–205.
- [22] J. St-Pierre, "PEMFC in situ liquid-water-content monitoring status," *J. Electrochem. Soc.*, vol. 154, no. 7, pp. B724–B731, 2007.
- [23] W. He, G. Lin, and T. V. Nguyen, "Diagnostic tool to detect electrode flooding in proton-exchange-membrane fuel cells," *AIChE J.*, vol. 49, no. 12, pp. 3221–3228, 2003.
- [24] F. Barbir, H. Gorgun, and X. Wang, "Relationship between pressure drop and cell resistance as a diagnostic tool for PEM fuel cells," *J. Power Sour.*, vol. 141, no. 1, pp. 96–101, 2005.
- [25] X. Yu, M. R. Starke, L. M. Tolbert, and B. Ozipneci, "Fuel cell power conditioning for electric power applications: A summary," *IET Electr. Power Appl.*, vol. 1, no. 5, pp. 643–656, Sep. 2007.
- [26] M. Shen, A. Joseph, J. Wang, F. Z. Peng, and D. J. Adams, "Comparison of traditional inverters and Z-source inverter for fuel cell vehicles," *IEEE Trans. Power Electron.*, vol. 22, no. 4, pp. 1453–1463, Jul. 2007.
- [27] N. Wagner and E. Gülzow, "Change of electrochemical impedance spectra (EIS) with time during CO-poisoning of the Pt-anode in a membrane fuel cell," *J. Power Sour.*, vol. 127, nos. 1–2, pp. 341–347, 2004.
- [28] H. Li *et al.*, "Impacts of operating conditions on the effects of chloride contamination on PEM fuel cell performance and durability," *J. Power Sour.*, vol. 218, pp. 375–382, Nov. 2012.
- [29] X.-Z. Yuan *et al.*, "Diagnosis of contamination introduced by ammonia at the cathode in a polymer electrolyte membrane fuel cell," *Int. J. Hydrogen Energy*, vol. 37, no. 17, pp. 12464–12473, 2012.
- [30] G. Dotelli, R. Ferrero, P. G. Stampino, and S. Latorrata, "Analysis and compensation of PEM fuel cell instabilities in low-frequency EIS measurements," *IEEE Trans. Instrum. Meas.*, doi: 10.1109/TIM.2013.2297632.
- [31] R. Ferrero, G. Dotelli, P. G. Stampino, and S. Latorrata, "Discussion of critical measurement issues of impedance spectroscopy on PEM fuel cells," in *Proc. IEEE AMPS 2012*, Aachen, Germany, Sep., pp. 97–102.

**Giovanni Dotelli** was born in Piacenza, Italy, in 1964. He received the M.Sc. degree in chemical engineering and the Ph.D. degree in materials engineering from Politecnico di Milano, Milano, Italy, in 1989 and 1993, respectively.

He has been an Associate Professor of Materials Science with the Department of Chemistry, Materials, and Chemical Engineering "G. Natta," Politecnico di Milano, since 2001, where he is in charge of the Laboratory of Materials for Energy and Environment. His current research interests include the materials for energy- and environmental-related sustainable technologies.

**Roberto Ferrero** (S'10–M'14) was born in Milano, Italy, in 1986. He received the M.Sc. and Ph.D. degrees in electrical engineering from Politecnico di Milano, Milano, Italy, in 2009 and 2013, respectively.

He has been a Temporary Research Fellow with the Department of Energy, Systems, Land and Constructions, University of Pisa, Pisa, Italy, since 2013. His current research interests include electrical measurements, in particular, applied to electromagnetic launchers and fuel cells.

**Paola Gallo Stampino** was born in Busto Arsizio, Italy, in 1974. She received the M.Sc. degree in material science from the University of Milano-Bicocca, Milano, Italy, and the Ph.D. degree in materials engineering from Politecnico di Milano, Milano, in 2002 and 2007, respectively.

She has been an Assistant Professor with the Department of Chemistry, Materials, and Chemical Engineering "G. Natta," Politecnico di Milano, since 2008. Her current research interests include synthesis and characterization of materials for energy and environment.

**Saverio Latorrata** was born in Taranto, Italy, in 1984. He received the M.Sc. degree in chemical engineering and the Ph.D. degree in materials engineering from Politecnico di Milano, Milano, Italy, in 2008 and 2014, respectively.

He was a Temporary Research Fellow with the Department of Chemistry, Materials and Chemical Engineering "G. Natta," Politecnico di Milano, until 2010. His current research interests include the development and characterization of innovative materials for PEM fuel cells.

**Sergio Toscani** (S'08–M'12) was born in Codogno, Italy, in 1983. He received the M.Sc. and Ph.D. degrees in electrical engineering from Politecnico di Milano, Milano, Italy, in 2007 and 2011, respectively.

He has been an Assistant Professor of Electrical and Electronic Measurements with Dipartimento di Elettronica, Informazione e Bioingegneria, Politecnico di Milano, since 2011. His current research interests include current and voltage transducers, electrical machine diagnostics, and characterization of electrical systems and components.